Reshuffling yeast chromosomes with CRISPR/Cas9

Aubin Fleiss[1], Samuel O'Donnell[1], Nicolas Agier[1], Stéphane Delmas[1] and Gilles Fischer[1, #]

[1]: Sorbonne Université, CNRS, Institut de Biologie Paris-Seine, Laboratory of Computational and Quantitative Biology, F-75005, Paris, France.

[#] corresponding author: Gilles Fischer gilles.fischer@sorbonne-universite.fr

ABSTRACT

Untangling the phenotypic impact of chromosomal rearrangements from the contribution of the genetic background requires versatile procedures to generate structural variations. We developed a CRISPR/Cas9-based method to efficiently reshuffle the yeast genome in a scarless and markerless manner. Simultaneously generating two double-strand breaks on different chromosomes and forcing the trans-chromosomal repair through homologous recombination by chimerical donor DNAs resulted reciprocal translocations at the base-pair resolution. We made these translocations either irreversible by deleting a small sequence at the junction or reversible to the original chromosomal configuration by inducing the backward translocation. Furthermore, generating multiple DSBs by targeting repeated sequences and using uncut copies of the repeats as template for trans-chromosomal repair resulted in a large diversity of karyotypes comprising multiple rearrangements including balanced and unbalanced variations. We validated the targeted translocations and characterized multiple rearrangements by long-read *de novo* genome assemblies. To test the phenotypic impact of rearranged chromosomes we first recapitulated in a lab strain the *SSU1/ECM34* translocation believed to provide increased sulphite resistance to wine isolates. Surprisingly, this resulted in decreased sulphite resistance in the reference strain showing that the sole translocation is not the driver of increased resistance. Secondly, we found that shuffled strains had severely impaired spore viability and showed large phenotypic diversity in various stressful conditions leading in some instances to a strong fitness advantage, although no coding region was altered by the rearrangements. Therefore our method allows exploring the genotypic space accessible by structural variations and their phenotypic impact independently from the background effect.

INTRODUCTION

Genetic polymorphisms are not restricted to base substitutions and indels but also include large-scale Structural Variations (SVs) of chromosomes. SVs comprise both unbalanced events, often designated as copy number variations (CNVs) including deletions and duplications, and balanced events that are copy number neutral and include inversions and translocations. Both have a phenotypic impact, however the prevalence and the fitness effect of balanced SVs has been less documented than CNVs, partly because they are much more challenging to map than CNVs and also because quantifying their fitness contribution independently from the confounding effect of base substitutions remains challenging. Natural balanced chromosomal rearrangements result from the exchange of DNA ends during the repair of Double Strand Breaks (DSBs) either through Homologous Directed Repair (HDR) between dispersed repeats or intact chromosomes carrying internal repeat sequences homologous to the DNA ends (Piazza et al. 2017), or through Non-Homologous End Joining (NHEJ) (Branzei and Foiani 2008). Artificial balanced rearrangements are classically engineered by inducing targeted DSBs and promoting repair through both HDR and NHEJ. However, inducing targeted DSBs and engineering scar-less chromosomal rearrangements has remained challenging. In early studies structural variants were obtained through I-SceI-induced DSB repair between split alleles of a selection marker (Fairhead et al. 1996; Richardson and Jasin 2000). In later developments, the use of the I-SceI endonuclease was combined to a “COunter-selectable REporter” or CORE cassette in the frame of the delitto-perfetto technique, allowing the generation of a reciprocal translocation in a scar-less fashion (Storici and Resnick, 2003, 2006). Other techniques based on Cre-Lox recombination were used to make the genomes of *Saccharomyces cerevisiae* and *Saccharomyces mikatae* colinear and generated interspecific hybrids that produced a large proportion of viable but extensively aneuploid spores (Delneri et al. 2003). Cre/Lox recombination was also used to assess the impact of balanced rearrangements in vegetative growth and meiotic viability (Naseeb and Delneri 2012; Avelar et al. 2013; Naseeb et al. 2016). A novel approach using yeast strains with synthetic chromosomes allowed extensive genome reorganization through CreLox-mediated chromosome scrambling (Annaluru et al. 2014; Hochrein et al. 2018; Jia et al. 2018; Shen et al. 2016). This approach proved to be efficient to generate strains with a wide variety of improved metabolic capacities (Jia et al. 2018; Blount et al. 2018; Luo et al. 2018b; Shen et al. 2018). Muramoto and collaborators recently developed a genome restructuring technology relying on a temperature-dependent endonuclease to conditionally introduce multiple rearrangements in the genome of *Arabidopsis thaliana* and *S. cerevisiae,* thus generating strains with marked phenotypes such as increased plant

biomass or ethanol production from xylose (Muramoto et al. 2018). Methods using Zinc Finger Nucleases (ZFNs) and Transcription Activator-Like Effector Nucleases (TALENs) were also developed to generate targeted rearrangement in yeast, mammalian and zebrafish cells (Brunet et al. 2009; Piganeau et al. 2013; Richard et al. 2014; Xiao et al. 2013). Although these technologies provide very useful insights, they are often difficult to implement and/or rely on the use of genetic markers. For this reason, the development of the CRISPR/Cas9 (Clustered Regularly Interspaced Short Palindromic Repeats/CRISPR associated) system has boosted the field of genome engineering (Doudna and Charpentier 2014; Fraczek et al. 2018; Alexander 2018). This system, initially derived from immune systems of bacteria, consists of an endonuclease encoded by the Cas9 gene of *Streptococcus pyogenes* and a short RNA that guides the endonuclease at the targeted genomic locus. The gRNA can be easily designed to target any genomic locus proximal to a “NGG” Promoter Adjacent Motif (PAM). This technology is now routinely used to introduce targeted DSBs in genomes from a wide variety of species (Wang and Qi, 2016). In yeast, CRISPR/Cas9 induced DSBs can be repaired with high efficiency by providing homologous repair DNA cassettes, allowing a variety of genome editions. Previous studies achieved the introduction of point mutations, single and multiple gene deletions and multiplexed genome modifications at different loci by transforming cells with plasmids bearing single or multiple gRNAs and linear DNA repair templates (DiCarlo et al. 2013; Jakočiūnas et al. 2015; Mans et al. 2015, 2018). CRISPR-based approaches have also been developed to add centromeres and telomeres to chromosome fragments (Sasano et al. 2016) concatenating chromosomes (Luo et al. 2018a; Shao et al. 2018) and for massively parallel genome editing to generate large libraries of genetic variants (Bao et al. 2015; Roy et al. 2018; Sadhu et al. 2017).

CRISPR/Cas9 also opened new avenues in the study of genome structure especially with the engineering of translocations in mammalian cells with high efficiency. The principle is to introduce two DSB in two distinct chromosome with CRISPR, then repair the DNA ends in trans by HDR with donor DNA carrying a selection marker, lost in a second step by Cre/Lox recombination leaving a single loxP element at the chromosomal junction (Vanoli et al. 2017).

In this study, we developed a CRISPR-Cas9 multiplexed genome editing strategy to generate markerless reversible and non-reversible reciprocal translocations in yeast with base-pair precision and high efficiency. We also induce multiple DSBs by targeting scattered Ty3-LTRs, thereby generating patchwork chromosomes resulting from multiple translocations and complex rearrangements. Finally, we quantified the phenotypic impacts

of both targeted and multiple rearrangements on meiotic fertility and mitotic growth in various stress conditions.

RESULTS

Rationale for chromosome reshuffling

We used a single-vector, pGZ110 (Bruce Futcher, personal communication), which encodes both the Cas9 nuclease gene and a gRNA expression cassette (fig 1). This cassette allows cloning of either a unique 20 bp fragment corresponding to the target sequence of the gRNA or a synthetic DNA fragment of 460 base-pairs reconstituting two different gRNAs in tandem (fig 1). This system is highly versatile as it allows cloning of any pair of gRNA in a single ligation step. Such pairs of gRNAs can induce two concomitant DSBs which, upon recombination with chimerical donor DNA, generate reciprocal translocations with a single-nucleotide precision when the DSBs are introduced in different chromosomes. Furthermore, a single gRNA that targets Long Terminal Repeats (LTRs) scattered on different chromosomes can induce a higher number of DSBs, eventually resulting in multiple rearrangements upon repair with the uncut LTR copies. All rearrangements are engineered in a scar-less fashion and without integrating any genetic marker in the genome.

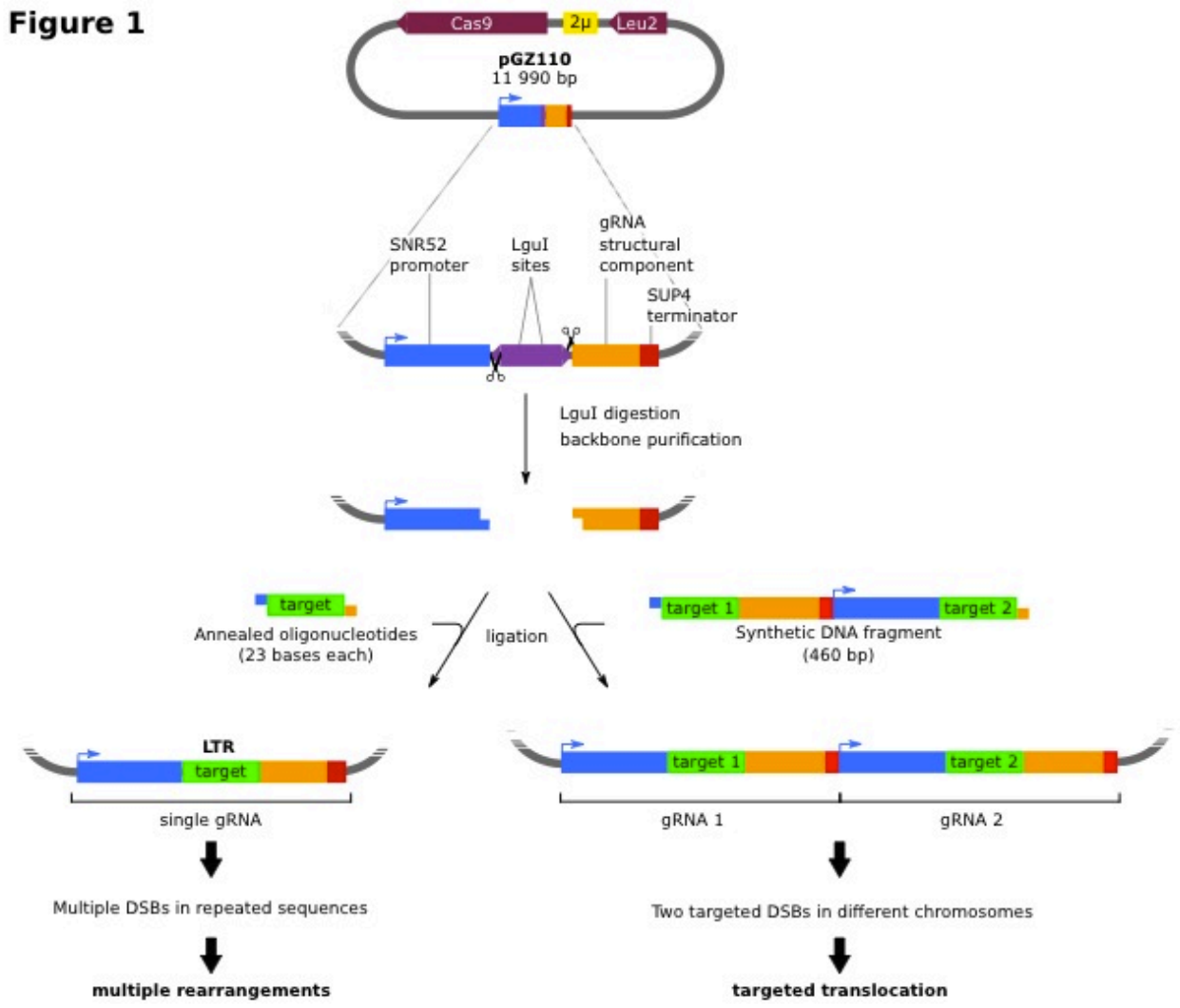

Figure 1: Experimental strategy to clone in one step a single or a pair of gRNA target sequences. The pGZ110 plasmid encodes the Cas9 nuclease under constitutive promoter TEF1p, the gRNA expression cassette and the LEU2 selection marker. The cassette consists of an SNR52 promoter (blue) separated from the structural component of the gRNA (orange) and a SUP4 terminator (red) by two divergently oriented LguI

sites (purple) allowing to clone the gRNA target sequence (green). Upon digestion, the two LguI sites generate non-complementary single strand overhangs of 3 bases. This system is highly versatile as it allows to clone in a single step either a 20 bp oligonucleotide corresponding to the target sequence of a unique gRNA (left) or a synthetic DNA fragment of 460 base-pairs reconstituting two different gRNA expression cassettes in tandem (right).

Engineering markerless, reversible reciprocal translocations at single base-pair resolution

We first engineered a reciprocal translocation between two reporter genes leading to phenotypes easy to observe upon disruption. Mutation in the *ADE2* gene involved in purine nucleotide biosynthesis results in the accumulation of a red pigment while mutating the *CAN1* gene which encodes an arginine permease confers canavanine resistance to the cells. We made this translocation reversible such that we can control the alternation between the two phenotypes [*ade2*,*can1*] and [*ADE2,CAN1*]. To generate two concomitant DSBs on chromosomes V and XV carrying *CAN1* and *ADE2*, respectively, we cloned two previously described gRNA target sequences, namely CAN1.Y and ADE2.Y (DiCarlo et al. 2013). To repair the DSBs, we co-transformed the cells with the plasmid bearing two gRNAs and "donor" DNA fragments of 90 base-pairs each composed of two homology regions of 45 bp identical to the sequences flanking CRISPR cutting sites (fig 2A upper). Two combinations of DNA repair donor fragments were used. As a control, we used donors called Point Mutation-donors (PM-donors), promoting the intra-chromosomal repair of DSBs in cis and mutating PAM sequences into stop codons, thus preventing further Cas9 activity. Besides, the donors promoting inter-chromosomal repair in trans, thus leading to a Reciprocal Translocation were called RT-donors. No point mutation needed to be introduced into the PAM sequence in this case because the translocation generates chimerical target sequences not complementary to the original gRNAs (fig 2A upper). Transformation with the plasmid bearing two gRNAs and either PM or RT-donors resulted in 89.1% and 95.1% of the colonies showing both the pink and resistance to canavanine phenotypes [*ade2*,*can1*], respectively (methods, fig 2B). We then tested by PCR the chromosomal junctions of 16 [*ade2*,*can1*] strains recovered from the RT experiment. The expected chimerical junctions were validated in all strains. We further validated the translocation by karyotyping two [*ade2*,*can1*] strains by PFGE. No other visible chromosomal rearrangements could be observed apart from the expected translocated chromosomes VtXV and XVtV (fig 2C). Sanger sequencing of 250 bp around the chimerical junctions of these two strains confirmed that the translocation occurred right at the position defined by the sequence of the RT-donors with no additional mutation (supp fig 1). Finally, we cured the plasmid from the two strains before performing the reverse translocation to restore *ADE2* and *CAN1* (Material and Methods).

Figure 2

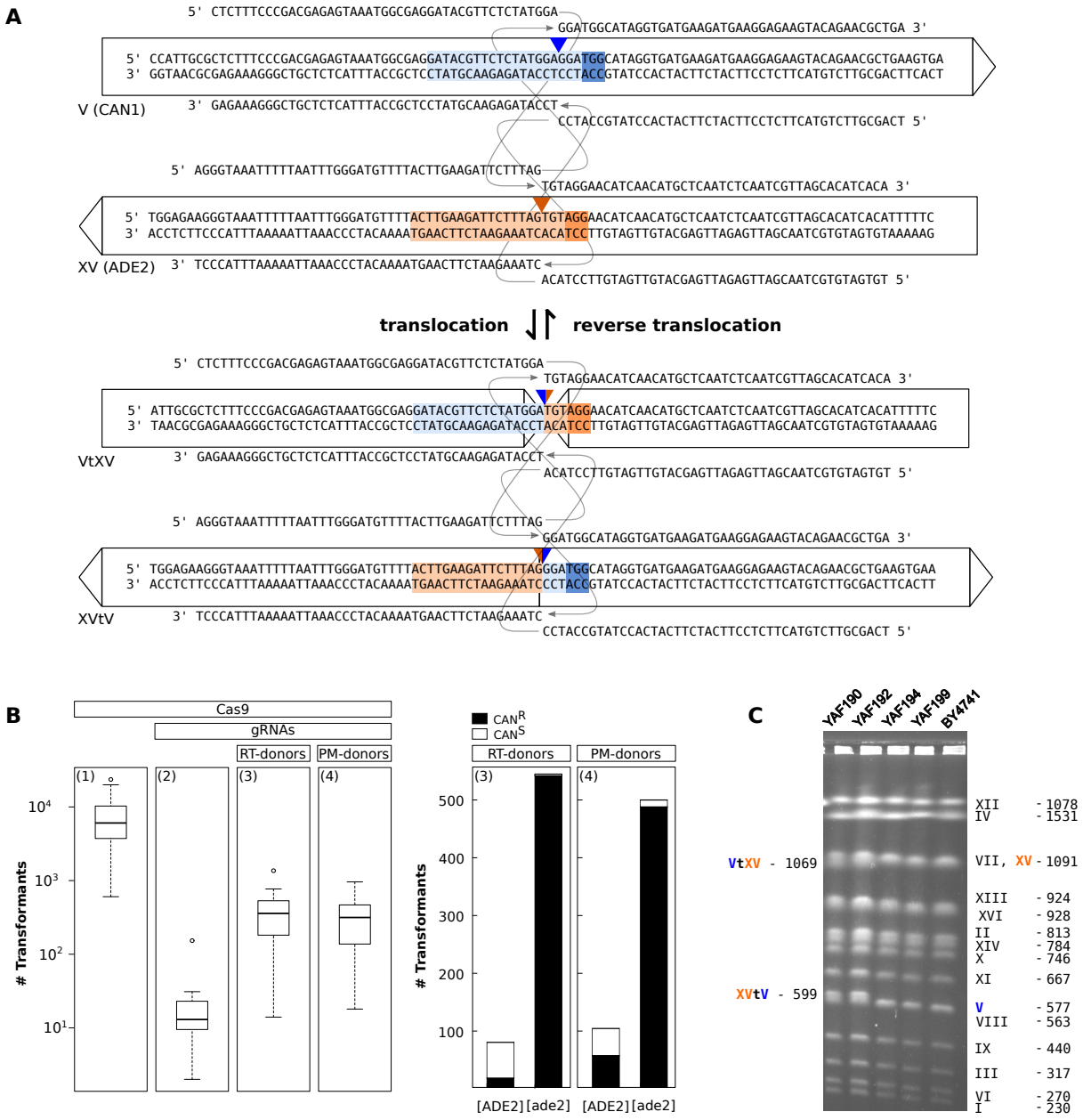

Figure 2: A Reversible markerless translocation. (A) The two gRNA target sequences are highlighted in light blue and orange. PAM sequences are highlighted in dark blue and orange. Triangles indicate DSBs sites. Arrows framing the sequences indicate the orientation of coding phases. Donor nucleotides are

represented above and below the frames by sequences linked by thin arrows to indicate their homology with the two different chromosomes. Top part: gRNAs and donors used to engineer the translocation between chromosomes V and XV at the ADE2 and CAN1 loci in BY4741, respectively; bottom part: gRNAs and donors used to revert the translocation between chromosomes VtVX and XVtV, thus restoring the natural junctions of BY4741. (B) Left: boxplots indicating the total number of transformants obtained in 16 independent transformation experiments. Panels (1) and (2) indicate efficient transformation with the Cas9 plasmid and high cutting efficiency of the gRNAs, respectively. Panels (3) and (4) show high mutation efficiency of the ADE2 locus by both the Reciprocal Translocation (RT) and Point Mutation (PM) donor DNAs used to repair the DSBs. Right: proportion of canavanine resistant (CANR) and sensitive (CANS) clones obtained in a total of 16 experiments with PM-donors (3) and RT-donors (4), showing that in both cases, more than 95.6% of [ade2] transformants are also mutated at the CAN1 locus. (C) PFGE karyotypes of two strains carrying the ADE2-CAN1 translocation (YAF190, YAF192) and two strains with restored chromosomes V and XV (YAF194 and YAF199 originating from YAF190 and YAF192, respectively). Chimerical chromosomes are denoted VtXV and XVtV. Original chromosome XV and V from the reference strain BY4741 are indicated in orange and blue respectively.

We cloned a pair of gRNAs that target the chimerical junctions formed by the *ADE2-CAN1* translocation in the Cas9 plasmid and designed repair donors to restore *ADE2* and *CAN1* to their original configuration (fig 2A, lower). Co-transformation with the gRNAs plasmid and donor fragments resulted in 94.2% of colonies which restored the white and canavanie sensitive phenotypes [*ADE2,CAN1*]. We performed pulse field electrophoresis karyotyping of 2 [*ADE2,CAN1*] strains. No difference could be observed between the karyotype of these two strains and that of the original BY4741 strain (fig 2C). The chromosomal junctions of the 2 de-translocated strains were Sanger-sequenced and were found identical to BY4741 natural junctions (supp fig 1). These results demonstrate that reversible chromosomal translocations can be engineered at base-pair resolution with high efficiency.

Engineering a deletion at the translocation breakpoint

In some instances, reciprocal translocations occur between repeated sequences (micro-homology or homologous sequences) that can also be used as template for the reverse translocation event restoring the WT configuration. Stabilizing a phenotype associated to an engineered translocation would therefore require the concomitant deletion of the homology regions to avoid such reversion events. We used our system to simultaneously generate a deletion of a few nucleotides and a reciprocal translocation. We used the same CAN1.Y and ADE2.Y gRNA target sequences as above and designed new donor fragments inducing deletions of 27 and 23 bp, including the PAM sequences, on chromosome V and XV, respectively (supp fig 2A). As above, we obtained a high proportion of [*ade2*,*can1*] transformants (96%). PCR of the junctions and karyotyping of 4 strains showed that chromosome V and XV underwent the expected reciprocal translocation (fig 3 A). The genome of one translocated strain was sequenced with Oxford Nanopore MinIon and *de-novo* assembled (Material and Methods, supp table 2 and 3). The translocated and reference genomes are collinear, except for chromosomes V and XV (fig. 3B). No other rearrangement is observed in

the translocated strain, suggesting no major off target activity of the Cas9 nuclease. In addition, the junction sequences are identical to the sequences of the chimerical donor fragments (supp fig 2B). These experiments demonstrate that a deletion and reciprocal translocation can be concomitantly engineered at base-pair resolution with CRISPR/Cas9 in the yeast genome.

Figure 3

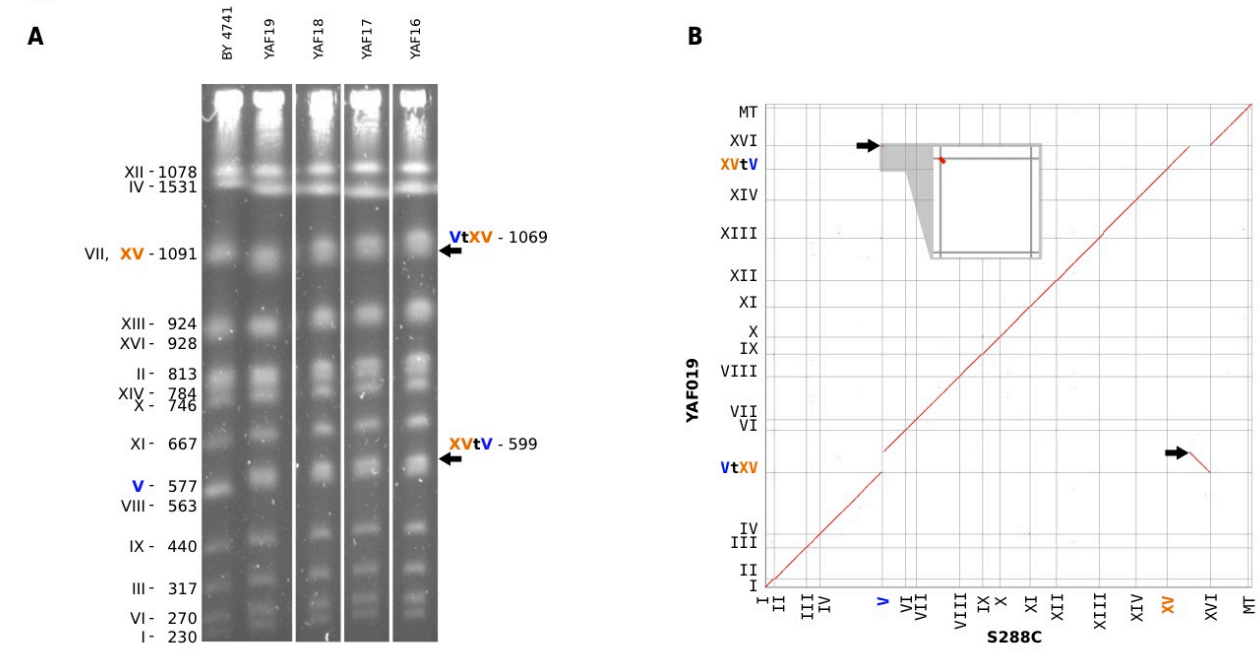

Figure 3: A non-reversible translocation between ADE2 and CAN1 genes. (A) PFGE karyotypes of 4 independent strains carrying the translocation (YAF16 to YAF19). All symbols are identical to Fig. 1C. (B) Homology matrix of de-novo assembled strain YAF019 vs S288c reference genome. Translocated fragments are indicated by black arrows.

Recapitulating a natural translocation involved in sulphite resistance in wine strains

It was previously reported that a reciprocal translocation between the promoters of *ECM34* and *SSU1*, a sulphite resistance gene, created a chimerical *SSU1-R* allele with enhanced expression resulting in increased resistance to sulphite in the wine strain Y9 (Perez-Ortin, 2002). This translocation resulted from a recombination event between 4 base-pair micro-homology regions on chromosomes VIII and XVI. We engineered the same translocation into the BY4741 background and tested sulphite resistance.

We first designed the two gRNA target sequences as close as possible to the micro-homology regions (supp fig 3A). The first gRNA targets the *SSU1* promoter region, 115 base-pairs upstream of the start codon. The second gRNA targets the promoter region of *ECM34*, 24 base-pairs upstream of the start codon (supp fig 3A). To mimic the translocated junctions present in the wine strains, we designed double stranded synthetic DNA donors of 90 base-pairs centered on the micro-homology regions but not on the cutting sites. In addition, each donor also contained a point mutation in the PAM sequences to prevent subsequent CRISPR recognition (supp fig 3A).

The transformation with the Cas9 plasmid containing the two gRNAs and the donor DNA yielded on average 202 transformants. We tested natural and chimerical junction by colony PCR for 16

transformants and found the expected chimerical junctions in 15 of them (supp fig 3B). This translocation was not visible by PFGE karyotyping because the size of the translocated chromosomes were too close to the size of the original chromosomes. To further validate the rearrangement, we checked the junctions by southern blot for one translocated strain with probes flanking the two cutting sites on chromosome VIII and XVI (fig 4A). This experiment clearly shows the presence of the chimerical junction fragments in the rearranged strain as compared to the WT. Finally, we sequenced the junctions of two translocated strains and found that the rearrangement occurred within the expected micro-homology regions. In addition, the system was designed such that both mutated PAMs ended up into the promoter of *ECM34*, therefore likely to have no impact on the expression of the sulphite resistance gene *SSU1* (supp fig 3C).

We then compared sulphite resistance between the lab strain in which we engineered the translocation, the non-translocated parental strain and wine isolates that either carry or are devoid of the translocation of interest. Surprisingly, we found that the engineered strain was the least resistant of all strains, including the non-translocated reference strain (fig 4B). This suggests that the promoter of *ECM34* in the BY background is weaker than the *SSU1* promoter. The wine isolate with the translocation was the most resistant, followed by the wine isolate without the translocation. It is interesting to note that the most resistant wine strain has tandem repeats of roughly 100bp in the promoter region of *SSU1* gene brought by the translocation with the original *ECM34* locus (Perez-Ortin, 2002). These repeats are absent from the reference strain.

Figure 4

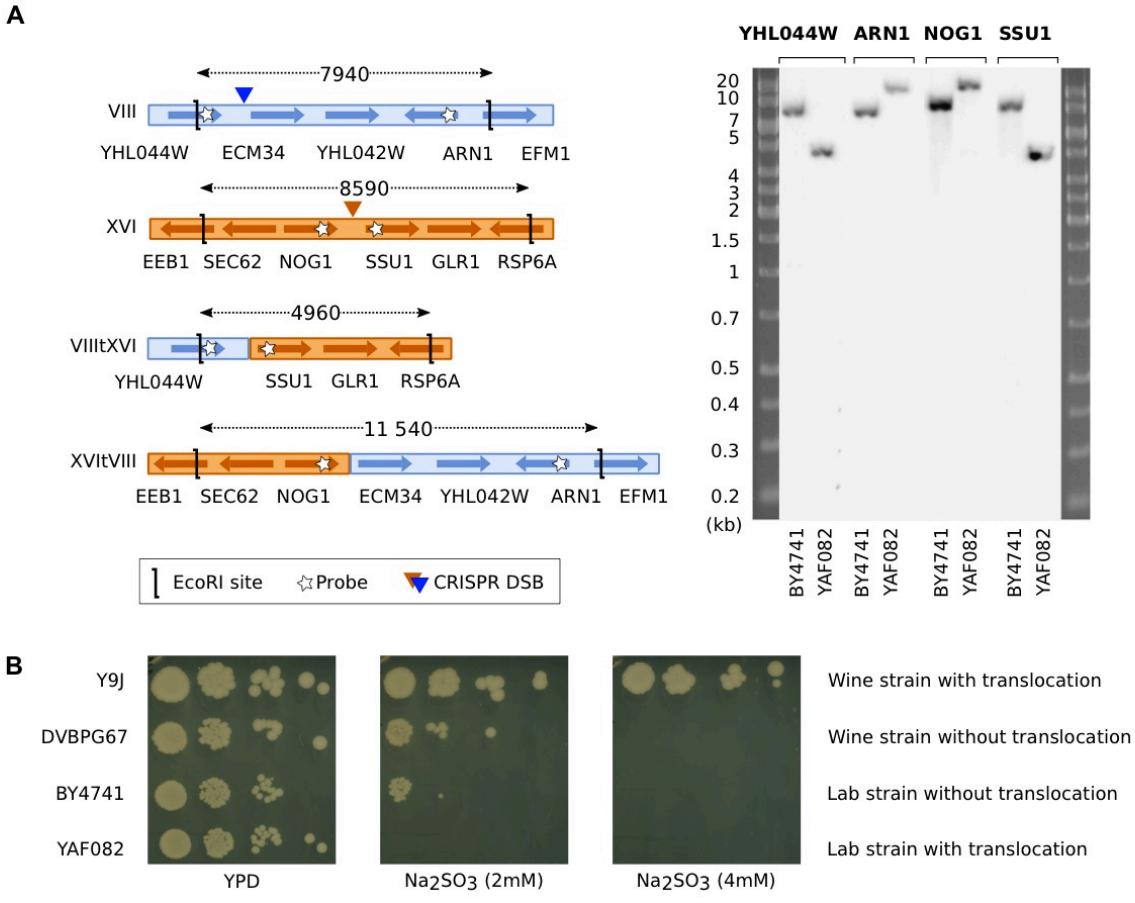

Figure 4: reciprocal translocation involved in sulphite resistance. (A) Left: schematic view of the chromosomal regions surrounding the translocation breakpoints. The double arrows indicate the length of the EcoRI restriction fragments. Right: Southern blot on the translocated strain YAF082 and parental strain BY4741. The probes are indicated on the top of the lanes. (B) Quantification of sulphite resistance of the strains Y9J, DVBPG6765, BY4741, YAF082 in the presence of 2 and 4 mM of Na2SO3.

Reshuffling chromosomes with multiple rearrangements

We introduced multiple DSBs in a single step using a unique gRNA targeting repeated Ty3 LTR sequences. There are 35 complete copies of Ty3 LTRs dispersed throughout the genome and these sequences are polymorphic (fig 5A, supp fig 4A). Four of them comprise a region identical to the gRNA target sequence and also contain a PAM. A fifth copy, also flanked by a PAM, differs from the target sequence by a single mismatch at its 5' end and therefore might also be recognized by the gRNA (supp fig 4A). These 5 copies are located in chromosomes IV, VII, XV and XVI (fig 5A). All the other Ty3 LTRs contain several mismatches or indels and/or are devoid of PAM, suggesting that Cas9 will not cut at these sites (supp fig 4A). Therefore, we expect from 1 to 5 sites to be concomitantly cut upon transformation with the Cas9/gRNA plasmid. In contrast to all experiments described above, we do not provide any donor DNA assuming that DSBs will be repaired by using uncut homologous LTR copies as template.

We transformed BY4741 and BY4742 cells with the Cas9/gRNA plasmid and recovered a total 211 and 159 transformants, respectively. We PFGE karyotyped 42 BY4741 and 36 BY4742 derived strains. Out of these, 39 strains showed clear chromosomal rearrangements on the gels with 29 different karyotypes (fig 5B). This result demonstrates that genomes are efficiently reshuffled by our strategy. Considering that all transformants must have repaired all DSBs and that all repaired chromosomes must be monocentric, we can predict 23 rearranged karyotypes (types B to X in supp fig 4B) as well as a WT-like karyotype that would result from DSB repair without any rearrangement (type A in supp fig 4B). In total 20 strains showed such predicted rearrangements, representing 11 distinct types (B, C, D, F, G, H, J, K, R, T and V in fig 5C). We validated the presence of all expected junctions by colony-PCR in 10 out of the 20 strains and on average 3 junctions out of 5 were also validated by PCR in the remaining 10 strains. We sequenced all chromosomal junctions in 2 strains that show the most frequently observed rearranged karyotype (type J in supp fig 4B). We found that all junctions, from both chimerical and un-rearranged chromosomes, were mutated in their PAM compared to the original target sequence (supp fig 4C). This shows that during shuffling, all targeted sites were cut and repaired using as donor other Ty3 LTRs that had no PAM. Additional mutations in the region corresponding to the gRNA target sequence were also observed for 3 junctions, but were too few to identify which copy of Ty3 LTR was used as donor (supp fig 4C). We compared the theoretical frequency of each possible junction in the predicted types, considering types B to X being equiprobable, with the observed frequency of the junctions in the predicted strains whose type was assigned by PFGE (fig 5D). We found very similar distributions, suggesting that DSBs were repaired in a random way. Moreover, we obtained

19 strains with 17 distinct unexpected karyotypes involving chromosomes other than the four targeted ones (fig 5B and 5C). For instance, chromosomes XI and XIV that have no PAM sequence associated with their Ty3 LTRs (supp fig 4A) are absent from several karyotypes suggesting that they can be rearranged in the absence of DSB (fig 5B). In addition, some of these unexpected karyotypes showed an apparent genome size increase suggesting the presence of large duplications (fig 5B). Using Oxford Nanopore MinION, we sequenced and *de-novo* assembled the genome of a strain showing a DNA content increase in PFGE (black star in fig 5B). We characterized in this strain an unequal reciprocal translocation between chromosomes VII and XV (fig 6A). The junctions corresponded to the targeted CRISPR cut site on chromosome XV but not on chromosome VII. In the chimerical chromosome XVtVII, the junction occurred away from the expected site resulting in a 30kb increase in DNA content (fig 6A). In the chimerical chromosome VIItXV, the junction also occurred away from the expected site but was accompanied by a truncated triplication of a 110 kb region. The missing part of the triplication corresponds to the 30 kb region found in the reciprocal chromosome XVtVII. The sequencing coverage relatively to the reference genome clearly confirmed the triplication of the complete 110 kb region (fig 6B). The displaced 30kb segment is referred to as region *a* and the other 80 kb segment as region *b*. In summary, one copy of region *a* lies at the chimerical junction of chromosome XVtVII, whereas the remaining two and three copies of region *a* and *b,* respectively, are found in tandem at the chimerical junction of chromosome VIItXV (fig 6C). Interestingly the 110kb segment, composed of regions *a* and *b*, is flanked by two Ty3 LTRs. Moreover, two full length Ty2 retrotransposons are found, one in chromosome XV directly flanking the targeted Ty3 LTR and the other one in chromosome VII at the junction between regions *a* and *b* (fig 6C).

Finally, we also recovered 39 type A strains that had a WT karyotype (fig 5C). For all of them we validated the presence of the un-rearranged junctions by colony PCR. We sequenced the junctions in 4 independent clones. Surprisingly, we found that these clones gather transformants that underwent two different paths within the same experiment. Firstly, 3 clones had junctions identical to the original LTR sequences with intact PAM, suggesting that Cas9 did not cut the target sites. Secondly, in the fourth clone, the PAM sequences of three junctions were mutated, showing that the corresponding chromosomes were cut and repaired yet without any rearrangement (supp fig 4C). In this clone, one junction could not be amplified, possibly because of a small-sized indel that could not be observed on the PFGE profile.

Figure 5

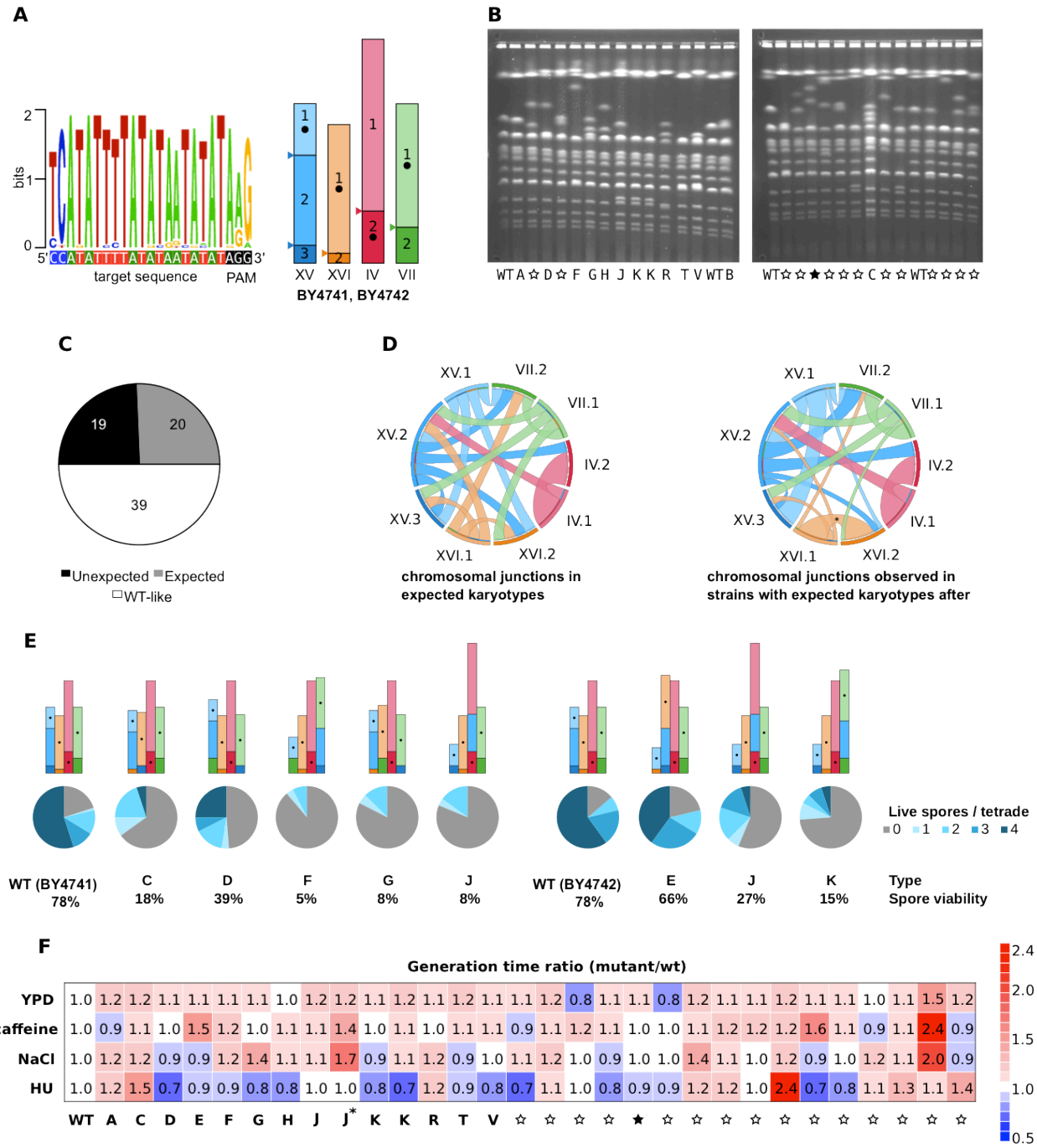

Figure 5: Induction of multiple rearrangements and phenotypic diversity of reshuffled strains. (A) Left: logo of the Ty3-LTR regions targeted by CRISPR/Cas9. The chosen target sequence is indicated below the logo with its associated PAM sequence in black. Right : Genomic location of the five LTR sequences that

best match the gRNA target sequence. Cutting sites are indicated by triangles. Chromosomes are represented proportionally to their size in kb. Centromeres are represented by black dots, not at their actual positions for readability (B) Twenty-six distinct karyotypes obtained by PFGE after after inducing multiple rearrangements, including type A, the wild-type-like. Letters indicate expected karyotypes (see supp fig 4B), that is, karyotypes explained by balanced rearrangements without change in DNA contents, when applicable. Unexpected karyotypes are indicated by a star. The strain with the black star has been sequenced (see fig 6). (C) Relative proportion of BY4741 and BY4742 derived strains with a WT like, predicted or unexpected karyotype. (D) Proportions of expected and observed chromosomal junctions. Left : theoretical frequency of chromosomal junctions in expected rearranged karyotypes (types B to X obtained by simulating the balanced repair of the 5 DSBs induced by CRISPR/Cas9 in Ty3-LTRs). Right : observed frequency of chromosomal junctions in type B to X as assigned by PFGE. The junction XVI.1-XVI.2, denoted by * is significantly enriched compared to the prediction (Chi2 conformity test with pval=0.03). (E) Percentage of viable spores and proportion of tetrads with 0, 1, 2, 3, 4 viable spores obtained from crosses between rearranged BY and WT SK1 strains. (F) Ratio between the generation times of rearranged strains and WT (columns) in various stress conditions (rows). Each ratio is the mean of 3 replicates. When applicable, the type of predicted strains is indicated at the bottom of the matrix, unexpected karyotypes are indicated by a star. J* denotes a type J strain where all junctions could not be validated by PCR.

Exploring the phenotypic diversity of reshuffled strains

Firstly, we tested the meiotic fertility of diploid strains heterozygous for the chromosomal rearrangements by measuring spore viability in their offspring (fig 5E). We tested 8 different strains with predicted karyotypes and PCR-validated junctions. These strains comprise various rearrangements including reciprocal translocations between 2 and 3 chromosomes (types C, D, E, F and G, respectively) and transpositions (types J and K). For each cross we dissected 10 tetrads from two independent diploid strains (20 tetrads in total). The control strain without any rearrangement shows 78% of viable spores with most tetrads harbouring 3 to 4 viable spores (fig 5E). By contrast, all heterozygous diploids had a severely impaired spore viability ranging from 5 to 39% with predominantly only 1 to 2 viable spores per tetrad, except one that shows 66% of spore viability (type E in fig 5E). We observed no clear correlation between the type of rearrangement and the impact on fertility. One strain with a single reciprocal translocation between 2 chromosomes (type F) shows the lowest viability, comparable to that of a more rearranged strain with 2 translocations between 3 chromosomes (type G). By contrast, the strain showing the highest spore viability also has a single translocation between two chromosomes (type E). Note that two strains carrying the same transposition (type J) but from opposite mating type present significantly different spore viabilities (Chi2 Pval=0.004) suggesting additional genotypic heterogeneities between the 2 strains or some interactions between the rearrangements and the genotypes of the parental strains. These results show that knowing the type of rearrangements is not sufficient to predict their quantitative impact on meiotic fertility, although most of them have a drastic negative effect.

Figure 6

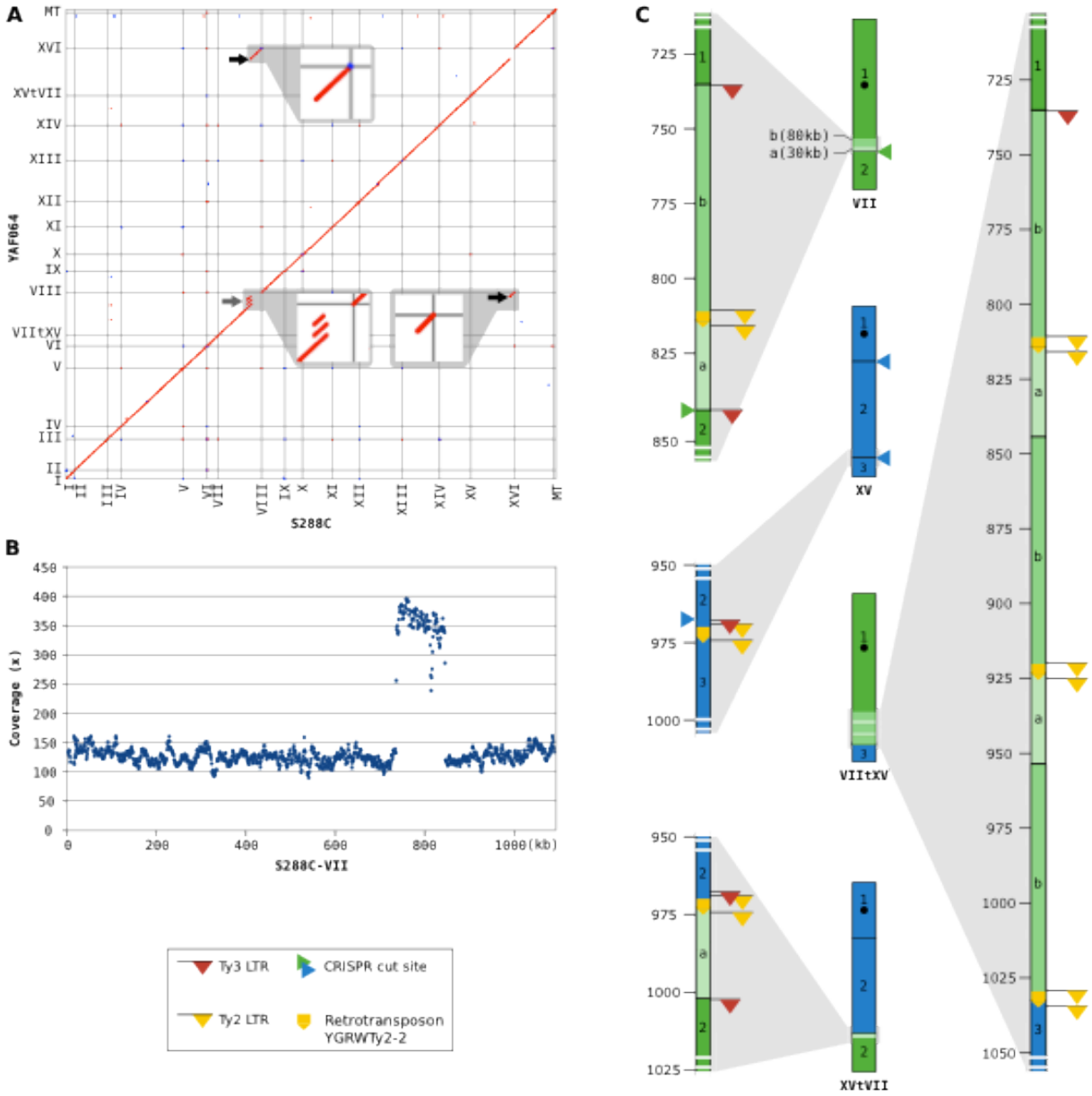

Figure 6: Genome with complex rearrangement. (A) Homology matrix between the genomes of the strain showing an increase in global DNA content in PFGE (YAF064) and S288c. Translocated fragments are indicated by black arrows. The tandem triplication at the junction of chromosome VIItXV is indicated by the

grey arrow. (B) Coverage of the YAF064 reads remapped on the reference chromosome VII. Each dot represents a window of 1kb. (C) Architecture of chromosomes VII (in green) and XV (in blue) of the reference strain and chimerical chromosomes VIItXV and XVtVII of the rearranged strain YAF064. Light grey triangles represent zoom-ins on chromosomal junctions. Ty3-LTRs and Ty2 LTRs elements are represented by red and yellow flags respectively. Full-length Ty2 elements are represented by yellow boxes. The Ty3 LTR copies targeted by CRISPR/Cas9 are indicated by green and blue triangles next to chromosomes VII and XV, respectively. Regions a and b, triplicated in the shuffled strain, are represented in lighter green shades.

Secondly, we measured the mitotic growth of rearranged strains in rich medium and under stress conditions including a variety of abiotic factors or drugs interfering with cell division. NaCl exerts an osmotic stress (Blomberg 1997), hydroxyurea (HU), is an inhibitor of nucleic acid synthesis (Koç et al. 2004), and caffeine is a cell-growth inhibitor known to interfere with the TOR pathway (Loewith and Hall 2011). We tested representative strains for 13 distinct predicted karyotype categories and 16 unexpected karyotype categories and indicated the generation time ratio of the rearranged mutants relatively to the WT strain (fig 5F). Note that the type A strain that has a WT-like karyotype showed either a generation time identical to the WT strain as expected or a slightly increased one (1.2 times, fig 5F). To be conservative, we decided to consider as significant only the values smaller than 0.8 and greater than 1.2. In rich medium, all but one rearranged strain show no significant growth difference than the WT, showing that chromosome reshuffling has little impact on mitotic fitness in this growth condition (from 1.0 to 1.2 times longer generation times) although in one case the rearrangements, involving extensive aneuploidy, proved highly disadvantageous (second strain on the right with a generation time ratio of 1.5). In both caffeine and NaCl conditions, 4 rearranged strains were negatively affected with the most impacted strain being also the slow grower in the rich medium (fig 5F). By contrast, in HU, the number of mutants positively and negatively impacted are much more balanced with 5 and 3 strains growing faster and slower than the WT, respectively. Interestingly, we found both predicted and unexpected karyotypes showing significant growth differences in the various environmental conditions with both positively and negatively impacted strains. In addition, two strains, one type G and one unexpected karyotype, showed alternatively increased and decrease mitotic fitness depending on the conditions showing genotype by environment interactions.

DISCUSSION

In this study, we developed a versatile CRISPR/Cas9-based method allowing to engineer, with the same efficiency as point mutations, both precisely target reciprocal translocations and multiple rearrangements. Cloning in a single step any two pair of gRNAs into a CRISPR/Cas9 vector allows generating any translocation at base-pair resolution on-demand. After the translocation, the new chromosomal junctions are not recognized by Cas9 which makes the incorporation of point mutation in the PAM sequence unnecessary. The preservation of an intact PAM sequence allows re-targeting the chimerical junctions by Cas9 and inducing the backward translocation restoring the original chromosomal configuration. Alternatively, introducing a small deletion at the translocation breakpoint ensures the stability of the rearranged configuration. Cloning in a single step a single gRNA that targets dispersed repeat sequences allows generating multiple chromosomal rearrangements simultaneously leading to a large diversity of karyotypes. Only one half of them could be explained by the expected repair in trans between the targeted DSBs (fig 5C). Considering that these predictable rearrangements were only represented by a small number of strains, some being not represented at all (supp fig 4B) and that the unexpected karyotypes were all nearly unique, the number of possible rearrangements accessible by our method is probably very large.

One reason that could explain some of the unexpected karyotypes would be that CRISPR/Cas9 may recognize and cut the two Ty3 LTRs on chromosome XII that contain a PAM despite small indels in the gRNA target sequence (supp fig 4A). Such types would be difficult to identify by PFGE because of the large size of chromosome XII and its frequent size variations due to the rDNA cluster dynamics. One cannot exclude that additional LTRs were cut by CRISPR/Cas9 even if this seems very unlikely because all other LTRs are devoid of PAM. A more plausible explanation would be multipartite ectopic recombination between cut and uncut chromosomes, as in (Piazza et al. 2017). In this study, the authors report that the single end of a DSB can invade multiple sequences located on intact chromosomes during its search for homology. This leads to translocations between intact chromosomes with insertions of fragments of the triggering single-end sequence in the translocation junctions. Consistently with this possibility we found that one unexpected chimerical junction resulted from Ty3-LTRs being “outcompeted” during repair by the full-length Ty2 elements found in the vicinity of the CRISPR-induced DSBs (fig 6). We also found several karyotypes with rearrangements in untargeted chromosomes suggesting that rearrangements can occur in intact chromosome in the absence of DSB.

Our procedure of genome reshuffling is reminiscent of the restructuring technology developed by Muramoto and collaborators (2018) that uses a temperature-dependent endonuclease to conditionally induce multiple DSBs in the genome of yeast and *A.thaliana*. However, our reshuffling procedure is potentially more versatile because we can target different types of repeated sequences with variable locations (within or between genes, subtelomeric or internal, etc) and variable copy numbers. By analyzing the genome of *S. cerevisiae* for repeated gRNA target sequences we identified 39,374 repeated targets with varying number of occurrences in the

genome (from 2 to 59). Repeated targets were mostly found within Ty transposable elements (11,503) and protein coding genes (10,368 in 479 genes located in all 16 chromosomes). Interestingly, we also found 3,438 repeated target gRNA located in intergenic regions which should allow to rearrange chromosomes without disrupting coding sequences. In addition, our CRISPR/Cas9 shuffling procedure is doable in any genetic background and therefore potentially more versatile than the Cre/Lox based SCRaMbLE techniques that can be used only in yeast strains with synthetic chromosomes.

Our approach provides the possibility to quantify the role of structural variants in organismal phenotypes. The translocation between the *SSU1* and *ECM34* genes provides increased sulphite resistance to wine isolates and is believed to be a consequence of sulphite supplementation in wine-making (Perez-Ortin, 2002). Surprisingly, the translocation we engineered in the reference strain resulted in decreased sulphite resistance. We hypothesize that this phenotype is linked to the absence of repeats in the promoter of *ECM34* in the BY4741 background in contrast to wine strains (Perez-Ortin, 2002), implying that the promoter of *ECM34* is weaker than the *SSU1* promoter in the BY background. Therefore, the translocation itself would not be sufficient to explain increased sulphite resistance. These findings provide a striking example of the advantages brought by our technique to untangle the phenotypic impact of SVs from that of the genetic background.

We also measured the phenotypes of strains carrying multiple rearrangements both in mitotic and meiotic conditions. We showed that crosses between rearranged and parental strains produced very few viable spores, supporting earlier studies revealing that meiotic pairing and segregation is impaired in diploid strains bearing heterozygous translocations (Avelar et al. 2013; Loidl et al. 1998; Liti et al. 2006). In vegetative growth, reshuffling provided a great phenotypic diversity with strains showing fitness advantages under specific environmental conditions. Similar findings were previously described both in *S. cerevisiae* (Naseeb et al. 2016; Colson et al. 2004) and *Schizosaccharomyces pombe* (Avelar et al. 2013). However, in our study all rearrangements are completely markerless and scarless (no CRE/Lox site) and no gene was disrupted nor duplicated (at least for the predicted karyotypes) suggesting that balanced rearrangements between repeated sequences simply reconfiguring the chromosome architecture are sufficient to create fitness diversity. Therefore, we believe that CRISPR/Cas9 chromosome reshuffling is a powerful new tool complementing the features of pre-existing genome restructuring technologies and will prove useful in the study of genotype to phenotype relationship and for isolating new chromosomal combinations of biotechnological interests.

METHODS

Strains and media

The strains of *Saccharomyces cerevisiae* BY4741, (*MATa*, *his3Δ1*, *leu2Δ0*, *ura3Δ0*, *met15Δ0*) and BY4742 (*MATα*, *his3Δ1*, *leu2Δ0*, *ura3Δ0*, *lys2Δ0*) were used for generating the translocations between the *ADE2* and *CAN1*, *ECM34* and *SSU1* genes, and for the multiple rearrangements. All pre-cultures were performed in YPD. After transformation, cells were selected on complete synthetic medium depleted in leucine (CSM-Leu). Plasmid cloning steps were performed in chemically competent *Escherichia coli* DH5α. Ampicillin resistant bacteria were selected on LB medium supplemented with ampicillin at 100 µg/ml. The SK1 strains 1513 (*MATα, ho::LYS2*, *ura3*, *leu2::HISG*, *lys2*, *arg4*(Nnde1)-Nsp, *thr1-A*, *SPO11*-HA3-His6::*KanMX4*) and 1708 (*MATa*, *ho::LYS2*, *ura3*, *leu2::HISG, lys2*, *arg4*-Bgl::NdeI-site1°, *CEN8::URA3*) provided by Bertrand Llorente (CRCM, Marseille) were used for their high sporulation efficiency compared to BY strains to perform crosses and to quantify spore viability of the rearranged strains. The sulphite resistance phenotype of our engineered strains was compared to that of wine strains Y9J_1b and DBVPG6765 provided by Joseph Schacherer (Université de Strasbourg).

Sulphite resistance spot tests

Sulphite resistance of two wine strains and two engineered lab strains (YAF082, YAF083) was assessed on YPD plates buffered at pH = 3.2 and supplemented with sulphites according to an established procedure (Park et al. 1999) with minor modifications: buffered plates were prepared by adding tartaric acid / potassium, sodium tartrate buffer to a final concentration of 38 mM to freshly autoclaved agar YPD. Sulphites plates were prepared by spreading a 1M stock solution of Na_2SO_3 on 75 ml buffered square plates to a final concentration of 2 mM or 4 mM. Sulphites were let to diffuse overnight at room temperature. The next day, for each experiment, we dispensed in triplicate 10^5, 10^4, 10^3, 10^2 cells of each strain in 50 µL sterile water drops. The position of each strain in the three replicates was different to minimize neighbouring and edge effects. The plates were incubated for 4 days at 30 °C before being scanned. The whole experiment was repeated 3 times.

Growth curves in stress conditions

Generation time of strains were measured under the following conditions: rich medium (YPD), salt stress (YPD + 1.5 M NaCl), inhibition of nucleic acid synthesis (YPD + hydroxyurea 20 mg/ml), presence of caffeine known as a toxic purine analogue (YPD + caffeine 16 mM). These drug concentrations impeding but not stopping cell growth were determined as the concentration required to generate an approximately three-fold increase in the generation time of BY4741 as compared to the YPD growth condition. Compared to the observed generation time of 80 minutes in YPD, there was a fold increase of 3.7, 3.85 and 2.8 in NaCl, Caffeine and HU conditions respectively. Cells were diluted from a saturated YPD culture to 2.10^6 cells/ml and 10 µl corresponding to 2.10^4 cells were used to inoculate a new plate with 90µl of fresh medium per well. OD_{600} measurement was performed in precision mode every 15 minutes for 3 days using the TECAN Sunrise micro-plate reader and Magellan v7.2 software. Constant high intensity “interior

mode" agitation and 30°C temperature were maintained during all experiments. In addition, a few Ø 500 µm glass beads (Sigma G8772) were added to each well to prevent cell aggregation. For each strain and condition, growth curves were carried out in triplicate and the generation time was extracted using the R growthcurver package and averaged on the three measurements.

Spore viability

Colonies of rearranged strains originating from the BY background and SK1 strains of the opposed mating type were mixed and spread on the same YPD plate and left overnight at 30°C. The next day, the cells were re-suspended in distilled water and single cells were picked using the Sanger MSM 400 micro-manipulator and left to grow on YPD for 2 days at 30°C until a colony appeared. Colonies originating from single cells were replicated on sporulation medium and left for 4 to 7 days at 30°C until tetrad appeared. For each cross, 10 tetrads from two diploid strains were dissected on YPD and left to grow for 3 days before counting viable spores.

Identification of CRISPR/Cas9 target sequences

For the translocation between *ADE2* and *CAN1*, the target sequences CAN.Y and ADE2.Y found in the literature (DiCarlo et al. 2013) were re-used. The new targets formed by the first translocation were targeted to "reverse" the translocation and restore the original junctions. For the *ECM34*/*SSU1* translocation, specific CRISPR/Cas9 target sequences with minimal off-targets were chosen as close as possible to the natural recombination site of wine strains with the CRISPOR v4.3 website (http://crispor.tefor.net) using the reference genome of *Saccharomyces cerevisiae* (UCSC Apr. 2011 SacCer_Apr2011/sacCer3) and the NGG protospacer adjacent motif. For multiple rearrangements, we identified 39 occurrences of Ty3-LTRs in the latest version of the genome of *Saccharomyces cerevisiae* S288C (accession number GCF_000146045.2), which we have aligned using MUSCLE. Four sequences were incomplete and excluded from further analysis. We then manually selected a suitable gRNA sequence targeting five Ty3-LTR elements and looked for off-targets to this target sequence with CRISPOR. Predicted off-targets had either mismatches with the chosen guide and/or were devoid of PAM indicating that they would not be recognized by CRISPR/Cas9.

Construction of CRISPR/Cas9 plasmids with one or two guides

All plasmids used in this study were obtained by cloning either 20bp, corresponding to the target sequence of a single gRNA, or a 460 bp synthetic DNA fragment allowing to reconstitute two gRNA expression cassettes in pGZ110 (fig 1). All oligonucleotides are listed in supp table 1. The plasmid pGZ110 was kindly provided by Gang Zhao and Bruce Futcher (Stony Brook University). We linearised pGZ110 with the enzyme LguI (ThermoFischer FD1934) and gel purified the backbone. In order to clone one target sequence we first annealed two oligonucleotides of 23 bases with adequate 5' overhangs of 3 bases to obtain the insert. Annealing was performed by mixing equimolar amounts of forward and reverse oligonucleotides at 100pmol/µl with NEBuffer 4 (New England Biolabs), heating 5 minutes at 95°C and allowing the mix to cool down slowly to room temperature. We then mixed 100ng of backbone with 20pmol of double stranded insert and performed the ligation with the Thermo Fischer Rapid DNA ligation Kit (K1422) according to

manufacturer instructions. In order to obtain plasmids with two gRNA expression cassettes, we first digested and gel-purified the 460bp synthetic DNA fragments with LguI to obtain inserts with adequate 5' overhangs of 3 bases for ligation in pGZ110. We then mixed 100ng of backbone and 20ng of insert and performed ligation as explained previously. Plasmids were amplified in *E. coli*. Oligonucleotides and synthetic DNA fragments were ordered from Eurofins. Refer to supplementary material for oligonucleotides and plasmid sequences.

Yeast transformation

Yeast cells were transformed using the standard lithium acetate method (Gietz and Woods 2002) with modest modifications : 10^8 cells per transformation were washed twice in 1mL of double distilled water, then washed twice in 1mL of 0.1x LiAc,TE before adding the T-mix and either donor-DNA or the equivalent volume of water and vortexing. Double-stranded donors for repair of CRISPR-induced DSBs were prepared beforehand by mixing equimolar amounts of forward and reverse oligonucleotides at 100pmol/µl with NEBuffer 4 (New England Biolabs), heating 5 minutes at 95°C and allowing the mix to cool down slowly to room temperature. Cells underwent a heat-shock of 25 minutes at 42°C. Centrifugation steps were performed at 9000 rpm with a tabletop centrifuge. After transformation, we checked for each transformation tube that the number of viable cells on YPD was comparable. Cells were re-suspended in distilled water, plated on leucine depleted medium and incubated 4 days at 30°C.

Plasmid Stability

The pGZ110 plasmid is highly unstable when selection is removed. To cure the plasmid cell were grown overnight in YPD at 30°C. Ten individual cells were micromanipulated on YPD plates with the MSM400 micromanipulator (Singer) and grown at 30°C for 2 days. Colonies were then serially replicated on CSM-Leu and YPD. All 10 colonies lost the ability to grow on CSM-Leu.

Estimation of CRISP/Cas9 cutting and repair efficiencies

The *ADE2*/*CAN1* experiment was used to quantify the translocation yields. We performed 16 independent transformation experiments. The transformations of 10^8 cells with the plasmid bearing no gRNA resulted in a median number of 6055 transformants, indicating high transformation efficiency. Transformation with the plasmid bearing two gRNAs but without providing any donor DNA for repair produced a median number of 12 transformants, indicating high cutting efficiency of 99.8% (fig 2). Co-transformation with the same plasmid and either PM or RT-donors provided median numbers of 315 and 358 transformants respectively, indicating high repair efficiencies both in cis and in trans. In total, PM-donor transformations provided 5360 colonies, 91.3% of which were pink [*ade2*]. We replicated 498 pink colonies on canavanine medium and 97,6% were resistant [*can1*]. In comparison only 53.9% of the 102 white transformants replicated on canavanine were resistant. RT-donor transformations provided in total 6735 colonies, 95,6% of which had acquired the pink phenotype. We then replicated 545 pink strains onto canavanine medium and 542 of them (99.5%) were resistant to canavanine. Also 20.5% of 78 white colonies replicated on canavanine medium were resistant (fig 2).

For the backward translocation restoring the ADE2/CAN1 original chromosomal configuration the transformation of two translocated strains with the plasmid bearing no gRNA produced on average 4010 colonies while cells transformed with the gRNAs plasmid but without donor DNAs produced on average 13 colonies, indicating efficient cutting of the chimerical junctions. Co-transformation with the gRNAs plasmid and donor fragments provided on average 207 colonies, 94.2% of which had the restored white phenotype. We replicated 16 white transformants on canavanine-supplemented medium and all strains were sensitive to canavanine.

Pulse Field Gel Electrophoresis and colony PCR for karyotyping rearranged strains

Whole yeast chromosomes agarose plugs were prepared according to a standard method (Török et al. 1993) and sealed in a 1% Seakem GTC agarose and 0.5x TBE gel. Pulse Field Gel Electrophoresis (PFGE) was conducted in with the CHEF-DRII (BioRad) system with the following program: 6V/cm for 10 hours with a switching time of 60 seconds followed by 6V/cm for 17h with switching time of 90 seconds. The included angle was 120° for the whole duration of the run. We compared observed karyotypes with expected chromosome sizes and tested the chromosomal junctions by colony PCR with ThermoFischer DreamTaq DNA polymerase.

Southern blot validation of *ECM34*/*SSU1* translocation

Southern blot was used to validate the translocation between *ECM34* (ch. VIII) and *SSU1* (ch. XVI). Genomic DNA was extracted from BY4741 and the engineered strain YAF082 using the Qiagen DNA buffer set (19060) and Genomic-tip 100/G (10243) according to manufacturer instructions and further purified and concentrated by isopropanol precipitation. Digestion of 10µg of genomic DNA per strain/probe assay was carried out using FastDigest EcoRI (ThermoFischer FD0274). Electrophoresis, denaturation and neutralisation of the gel were performed according to established procedure (Sambrook et al. 1989). Transfer on nylon membrane (Amersham Hybond XL) was performed using the capillarity setup (Khandjian, 1987; Southern, 1975). The membrane was UV-crosslinked with the Stratalinker 1800 device in automatic mode. Probes targeting the genes YHL044W and *ARN1* located upstream and downstream of the cutting site in the *ECM34* promoter respectively and the genes *NOG1* and *SSU1* located upstream and downstream of the cutting site in the *SSU1* promoter respectively were amplified with ThermoFischer DreamTaq, DIG-11-dUTP deoxyribonucleotides (Roche 11 175 033 910) and gel purified. Blotting and revelation were conducted using the Roche DIG High Prime DNA Labelling and Detection Starter kit II (11 585 614 910) according to manufacturer instructions. Imaging was performed using the G:BOX Chemi XT4 (Syngene) with CSPD chemiluminescence mode. All oligonucleotides are described in supp table 1.

Oxford Nanopore *de-novo* genome assembly

DNA from strains YAF019 and YAF064 was extracted using QIAGEN Genomic-tip 20/G columns and sheared using covaris g-TUBEs for average reads lengths of 8kb and 15kb respectively. DNA was repaired and dA-tailed using PreCR and FFPE kits (New England Biolabs) and cleaned with Ampure XP beads (Beckman Coulter). SQK-LSK108 adapters were ligated and libraries run on

FLO-MIN107 R9.5 flowcells. Raw signals were basecalled locally using Albacore v2.0.2 with default quality filtering. Flowcell outputs are shown in supp table 2.

YAF019 was assembled using the LRSDAY v1 pipeline (Yue and Liti, Nature Protocols, 2018) , including nanopolish v0.8.5 correction and excluding pilon polishing due to lack of illumina data. Due to only 19x coverage, the correctedErrorRate for Canu assembly was increased to 0.16. Assembly data are shown in supp table 3.

YAF064 was processed using the LRSDAY v1 pipeline. Linear chromosomes were assembled by SMARTdenovo v1 using 40x coverage of the longest Canu-corrected reads and combined with a Canu assembled mitochondrial genome. For canu correction, due to 200x coverage, correctedErrorRate was set at 0.75. All corrected reads were aligned against a reference-quality S288C genome, assembled with PacBio reads (Yue et al. 2017) using LAST-921. Split reads were used to highlight structural variations not apparent in the SMARTdenovo assembly. Read coverage was used to calculate an increase in the number of copies of particular regions within the rearranged genome. Evidence of rearrangements defined by overlapping reads and changes in copy number were used to manually adjust the assembly prior to nanopolish v0.8.5 and Pilon v1.22 error correction.

DATA ACCESS

The Oxford Nanopore sequencing data are deposited in the Sequence Read Archive under the project number (accession number pending).

ACKNOWLEDGMENTS

We thank our colleagues, Gianni Liti (IRCAN, France) and Joseph Schacherer (Université de Strasbourg, France) for fruitful discussions and constructive suggestions. We are grateful to Bruce Futcher and Gang Zhao (Stony Brook University, USA) for providing the pGZ110 plasmid and to Bertrand Llorente (CRCM, France) and Joseph Schacherer for the SK1 and wine strains, respectively. We are also grateful to Maëlys Born-Bony for her experimental help and to the 'Biologie Moléculaire et Cellulaire' Master students from Sorbonne Université who performed transformation experiments during their practical in the frame of the teaching module called 'Biologie synthetique et ingenierie des genomes' (4V150). This work was supported by the Agence Nationale de la Recherche [ANR-16-CE12-0019].

REFERENCES

Alexander WG. 2018. A history of genome editing in Saccharomyces cerevisiae. *Yeast Chichester Engl* **35**: 355–360.

Annaluru N, Muller H, Mitchell LA, Ramalingam S, Stracquadanio G, Richardson SM, Dymond JS, Kuang Z, Scheifele LZ, Cooper EM, et al. 2014. Total Synthesis of a Functional Designer Eukaryotic Chromosome. *Science* **344**: 55–58.

Avelar AT, Perfeito L, Gordo I, Ferreira MG. 2013. Genome architecture is a selectable trait that can be maintained by antagonistic pleiotropy. *Nat Commun* **4**: 2235.

Bao Z, Xiao H, Liang J, Zhang L, Xiong X, Sun N, Si T, Zhao H. 2015. Homology-Integrated CRISPR–Cas (HI-CRISPR) System for One-Step Multigene Disruption in *Saccharomyces cerevisiae*. *ACS Synth Biol* **4**: 585–594.

Blount BA, Gowers G-OF, Ho JCH, Ledesma-Amaro R, Jovicevic D, McKiernan RM, Xie ZX, Li BZ, Yuan YJ, Ellis T. 2018. Rapid host strain improvement by in vivo rearrangement of a synthetic yeast chromosome. *Nat Commun* **9**. http://www.nature.com/articles/s41467-018-03143-w (Accessed July 19, 2018).

Branzei D, Foiani M. 2008. Regulation of DNA repair throughout the cell cycle. *Nat Rev Mol Cell Biol* **9**: 297–308.

Brunet E, Simsek D, Tomishima M, DeKelver R, Choi VM, Gregory P, Urnov F, Weinstock DM, Jasin M. 2009. Chromosomal translocations induced at specified loci in human stem cells. *Proc Natl Acad Sci* **106**: 10620–10625.

Colson I, Delneri D, Oliver SG. 2004. Effects of reciprocal chromosomal translocations on the fitness of Saccharomyces cerevisiae. *EMBO Rep* **5**: 392–398.

Delneri D, Colson I, Grammenoudi S, Roberts IN, Louis EJ, Oliver SG. 2003. Engineering evolution to study speciation in yeasts. *Nature* **422**: 68–72.

DiCarlo JE, Norville JE, Mali P, Rios X, Aach J, Church GM. 2013. Genome engineering in Saccharomyces cerevisiae using CRISPR-Cas systems. *Nucleic Acids Res* **41**: 4336–4343.

Doudna JA, Charpentier E. 2014. The new frontier of genome engineering with CRISPR-Cas9. *Science* **346**: 1258096–1258096.

Fairhead C, Llorente B, Denis F, Soler M, Dujon B. 1996. New vectors for combinatorial deletions in yeast chromosomes and for gap-repair cloning using "split-marker" recombination. *Yeast Chichester Engl* **12**: 1439–1457.

Fraczek MG, Naseeb S, Delneri D. 2018. History of genome editing in yeast. *Yeast* **35**: 361–368.

Hochrein L, Mitchell LA, Schulz K, Messerschmidt K, Mueller-Roeber B. 2018. L-SCRaMbLE as a tool for light-controlled Cre-mediated recombination in yeast. *Nat Commun* **9**. http://www.nature.com/articles/s41467-017-02208-6 (Accessed July 19, 2018).

Jakočiūnas T, Bonde I, Herrgård M, Harrison SJ, Kristensen M, Pedersen LE, Jensen MK, Keasling JD. 2015. Multiplex metabolic pathway engineering using CRISPR/Cas9 in Saccharomyces cerevisiae. *Metab Eng* **28**: 213–222.

Jia B, Wu Y, Li B-Z, Mitchell LA, Liu H, Pan S, Wang J, Zhang H-R, Jia N, Li B, et al. 2018. Precise control of SCRaMbLE in synthetic haploid and diploid yeast. *Nat Commun* **9**: 1933.

Koç A, Wheeler LJ, Mathews CK, Merrill GF. 2004. Hydroxyurea Arrests DNA Replication by a Mechanism That Preserves Basal dNTP Pools. *J Biol Chem* **279**: 223–230.

Liti G, Barton DBH, Louis EJ. 2006. Sequence Diversity, Reproductive Isolation and Species Concepts in Saccharomyces. *Genetics* **174**: 839–850.

Loewith R, Hall MN. 2011. Target of Rapamycin (TOR) in Nutrient Signaling and Growth Control. *Genetics* **189**: 1177–1201.

Loidl J, Jin QW, Jantsch M. 1998. Meiotic pairing and segregation of translocation quadrivalents in yeast. *Chromosoma* **107**: 247–254.

Luo J, Sun X, Cormack BP, Boeke JD. 2018a. Karyotype engineering by chromosome fusion leads to reproductive isolation in yeast. *Nature* **560**: 392–396.

Luo Z, Wang L, Wang Y, Zhang W, Guo Y, Shen Y, Jiang L, Wu Q, Zhang C, Cai Y, et al. 2018b. Identifying and characterizing SCRaMbLEd synthetic yeast using ReSCuES. *Nat Commun* **9**. http://www.nature.com/articles/s41467-017-00806-y (Accessed July 19, 2018).

Mans R, van Rossum HM, Wijsman M, Backx A, Kuijpers NGA, van den Broek M, Daran-Lapujade P, Pronk JT, van Maris AJA, Daran J-MG. 2015. CRISPR/Cas9: a molecular Swiss army knife for simultaneous introduction of multiple genetic modifications in Saccharomyces cerevisiae. *FEMS Yeast Res* **15**. https://academic.oup.com/femsyr/article-lookup/doi/10.1093/femsyr/fov004 (Accessed August 14, 2017).

Mans R, Wijsman M, Daran-Lapujade P, Daran J-M. 2018. A protocol for introduction of multiple genetic modifications in Saccharomyces cerevisiae using CRISPR/Cas9. *FEMS Yeast Res*. https://academic.oup.com/femsyr/advance-article/doi/10.1093/femsyr/foy063/5026622 (Accessed July 19, 2018).

Muramoto N, Oda A, Tanaka H, Nakamura T, Kugou K, Suda K, Kobayashi A, Yoneda S, Ikeuchi A, Sugimoto H, et al. 2018. Phenotypic diversification by enhanced genome restructuring after induction of multiple DNA double-strand breaks. *Nat Commun* **9**: 1995.

Naseeb S, Carter Z, Minnis D, Donaldson I, Zeef L, Delneri D. 2016. Widespread Impact of Chromosomal Inversions on Gene Expression Uncovers Robustness via Phenotypic Buffering. *Mol Biol Evol* **33**: 1679–1696.

Naseeb S, Delneri D. 2012. Impact of Chromosomal Inversions on the Yeast DAL Cluster ed. J. Mata. *PLoS ONE* **7**: e42022.

Park H, Lopez NI, Bakalinsky AT. 1999. Use of sulfite resistance in Saccharomyces cerevisiae as a dominant selectable marker. *Curr Genet* **36**: 339–344.

Piazza A, Wright WD, Heyer W-D. 2017. Multi-invasions Are Recombination Byproducts that Induce Chromosomal Rearrangements. *Cell* **170**: 760-773.e15.

Piganeau M, Ghezraoui H, De Cian A, Guittat L, Tomishima M, Perrouault L, Rene O, Katibah GE, Zhang L, Holmes MC, et al. 2013. Cancer translocations in human cells induced by zinc finger and TALE nucleases. *Genome Res* **23**: 1182–1193.

Richard G-F, Viterbo D, Khanna V, Mosbach V, Castelain L, Dujon B. 2014. Highly Specific Contractions of a Single CAG/CTG Trinucleotide Repeat by TALEN in Yeast ed. T. Ashizawa. *PLoS ONE* **9**: e95611.

Richardson C, Jasin M. 2000. Frequent chromosomal translocations induced by DNA double-strand breaks. *Nature* **405**: 697–700.

Roy KR, Smith JD, Vonesch SC, Lin G, Tu CS, Lederer AR, Chu A, Suresh S, Nguyen M, Horecka J, et al. 2018. Multiplexed precision genome editing with trackable genomic barcodes in yeast. *Nat Biotechnol*. https://www.nature.com/articles/nbt.4137 (Accessed May 12, 2018).

Sadhu MJ, Bloom JS, Day L, Siegel JJ, Kosuri S, Kruglyak L. 2017. Highly parallel genome variant engineering with CRISPR/Cas9 in eukaryotic cells. http://biorxiv.org/lookup/doi/10.1101/147637 (Accessed August 14, 2017).

Sambrook J, Fritsch EF, Maniatis T. 1989. *Molecular cloning: a laboratory manual.* Cold Spring Harbor Laboratory Press, Cold Spring Harbor, NY, USA.

Sasano Y, Nagasawa K, Kaboli S, Sugiyama M, Harashima S. 2016. CRISPR-PCS: a powerful new approach to inducing multiple chromosome splitting in Saccharomyces cerevisiae. *Sci Rep* **6**. http://www.nature.com/articles/srep30278 (Accessed July 19, 2018).

Shao Y, Lu N, Wu Z, Cai C, Wang S, Zhang L-L, Zhou F, Xiao S, Liu L, Zeng X, et al. 2018. Creating a functional single-chromosome yeast. *Nature* **560**: 331–335.

Shen MJ, Wu Y, Yang K, Li Y, Xu H, Zhang H, Li B-Z, Li X, Xiao W-H, Zhou X, et al. 2018. Heterozygous diploid and interspecies SCRaMbLEing. *Nat Commun* **9**: 1934.

Shen Y, Stracquadanio G, Wang Y, Yang K, Mitchell LA, Xue Y, Cai Y, Chen T, Dymond JS, Kang K, et al. 2016. SCRaMbLE generates designed combinatorial stochastic diversity in synthetic chromosomes. *Genome Res* **26**: 36–49.

Török T, Rockhold D, King AD. 1993. Use of electrophoretic karyotyping and DNA-DNA hybridization in yeast identification. *Int J Food Microbiol* **19**: 63–80.

Vanoli F, Tomishima M, Feng W, Lamribet K, Babin L, Brunet E, Jasin M. 2017. CRISPR-Cas9–guided oncogenic chromosomal translocations with conditional fusion protein expression in human mesenchymal cells. *Proc Natl Acad Sci* **114**: 3696–3701.

Xiao A, Wang Z, Hu Y, Wu Y, Luo Z, Yang Z, Zu Y, Li W, Huang P, Tong X, et al. 2013. Chromosomal deletions and inversions mediated by TALENs and CRISPR/Cas in zebrafish. *Nucleic Acids Res* **41**: e141–e141.

Yue J-X, Li J, Aigrain L, Hallin J, Persson K, Oliver K, Bergström A, Coupland P, Warringer J, Lagomarsino MC, et al. 2017. Contrasting evolutionary genome dynamics between domesticated and wild yeasts. *Nat Genet* **49**: 913–924.